

Chapter 4

One-sided Process Capability Assessment in the Presence of Gauge Measurement Errors

In the manufacturing industry, many product characteristics are of one-sided specifications. The process capability indices C_{PU} and C_{PL} are often used to measure process performance (see equation (1.2)). The index C_{PU} measures the capability of a smaller-the-better process with an upper specification limit USL , whereas the index C_{PL} measures the capability of a larger-the-better process with a lower specification limit LSL . If the quality characteristic of manufacturing process is normally distributed, the process yield can be expressed by

$$\%yeild = \Phi(3C_I), \quad (4.1)$$

where Φ is the cumulative distribution function of the standard normal distribution, and $C_I = C_{PU}$ or C_{PL} . It is clear that the relationship between the index C_I and process yield is one-to-one. Thus, the index C_I provides an exact measure of process yield. Table 8 displays some commonly used capability values of C_I , the corresponding process yield, and nonconformity units in parts per million (NCPMM).

Montgomery [31] recommended some minimum quality requirements on C_I . For existing processes, the capability must be no less than 1.25, and for new processes, the capability must be no less than 1.45. For existing processes on safety, strength, or critical parameters, the capability must be no less than 1.45, and for new processes on safety, strength, or critical parameters, the capability must be no less than 1.60. Using the index C_I , the practitioners can evaluate their process capability and make decisions.

Table 8. The corresponding process yield and NCPMM for C_I .

C_I	Process yield (%)	NCPMM
1.00	0.9986501020	1350
1.33	0.9999669634	33
1.50	0.9999966023	3.4
1.67	0.9999997278	0.272
2.00	0.9999999990	0.001

In section 4.1, we discuss the relationship between the empirical process capability C_I^y and the true process capability C_I . In section 4.2, we obtain the pdf, the expected value, the variance and the MSE of \tilde{C}_I^y . And, we compare the MSE of \tilde{C}_I^y with that of \tilde{C}_I . In section 4.3, we use the confidence interval bounds

in Pearn & Shu [40] to estimate the minimum process capability by \tilde{C}_I^Y , we show that a large measurement error results in significantly underestimating the true process capability. In section 4.4, we use the critical values in Pearn & Chen [35] to test whether the process capability meets the requirement, and we show that the α -risk and the power both become decrease with measurement error. In section 4.5, we present our modified confidence interval bounds and critical values for the cases that measurement errors are unavoidable. Finally in section 4.6, an example is presented.

4.1 Empirical Process Capability C_I^Y

Suppose that $X \sim \text{Normal}(\mu, \sigma^2)$ represents the relevant quality characteristic of a manufacturing process, Mittag [27] introduced the degree of error contamination, $\tau = \sigma_M / \sigma$. The relationship between the empirical process capability index C_I^Y and the true process capability index C_I is

$$\frac{C_I^Y}{C_I} = \frac{1}{\sqrt{1+\tau^2}}, \quad (4.2)$$

where C_{PU}^Y or C_{PL}^Y is denoted here as C_I^Y . Since the variation of the empirical data we observe is greater than the variation of the original data, the denominator of the index C_I becomes larger, and we would understate the true capability of the process if we calculate the process capability based on the empirical data.

In Table 9, we tabulate some empirical process capabilities with $\tau = 0(0.1)1.0$ for various true process capability $C_I = 0.50, 1.00, 1.33, 1.50, 1.67, 2.00$, and 2.50 . If $\tau = 1.0$, then for $C_I^Y = 0.35$ the true process capability is $C_I = 0.50$, and for $C_I^Y = 1.77$ the true process capability $C_I = 2.50$. The empirical process capability diverges from the true one more when the measurement error increases. It is obvious that the gauge accuracy is less important if the required process capability is only marginally capable, and becomes more critical as the true capability requirement gets more stringent.

Table 9. Process capability with $\tau = 0(0.1)1.0$ for various C_I .

C_I	τ									
	0.1	0.2	0.3	0.4	0.5	0.6	0.7	0.8	0.9	1.0
0.50	0.50	0.49	0.48	0.46	0.45	0.43	0.41	0.39	0.37	0.35
1.00	1.00	0.98	0.96	0.93	0.89	0.86	0.82	0.78	0.74	0.71
1.33	1.32	1.30	1.27	1.23	1.19	1.14	1.09	1.04	0.99	0.94
1.50	1.49	1.47	1.44	1.39	1.34	1.29	1.23	1.17	1.11	1.06
1.67	1.66	1.64	1.60	1.55	1.49	1.43	1.37	1.30	1.24	1.18
2.00	1.99	1.96	1.92	1.86	1.79	1.71	1.64	1.56	1.49	1.41
2.50	2.49	2.45	2.39	2.32	2.24	2.14	2.05	1.95	1.86	1.77

4.2 Sampling Distribution of \tilde{C}_I^Y

Since the process parameters μ and σ are unknown, we therefore cannot evaluate the actual process capability. But, given sample data taken from the process, we could estimate process capability. Denoting $\{X_i, i=1, \dots, n\}$ the random sample of size n from the quality characteristics X , the natural estimators of C_{PU} and C_{PL} are

$$\hat{C}_{PU} = \frac{USL - \bar{X}}{3S}, \quad \hat{C}_{PL} = \frac{\bar{X} - LSL}{3S}, \quad (4.3)$$

where $\bar{X} = \sum_{i=1}^n X_i / n$ and $S = [\sum_{i=1}^n (X_i - \bar{X})^2 / (n-1)]^{1/2}$ are conventional estimators of μ and σ . Assume that X and M are stochastically independent, $Y \sim \text{Normal}(\mu, \sigma_Y^2 = \sigma^2 + \sigma_M^2)$. With a given sample $\{Y_i, i=1, \dots, n\}$, the estimators of C_{PU} and C_{PL} are

$$\tilde{C}_{PU}^Y = b_{n-1} \frac{USL - \bar{Y}}{3S_Y}, \quad \tilde{C}_{PL}^Y = b_{n-1} \frac{\bar{Y} - LSL}{3S_Y}, \quad (4.4)$$

Based on the same argument used in Chou & Owen [6] and Pearn & Chen [35], the estimator \tilde{C}_I^Y (\tilde{C}_{PU}^Y or \tilde{C}_{PL}^Y) is distributed as $dt_{n-1}(\delta^Y)$, where $d = b_{n-1}(3\sqrt{n})^{-1}$ and $t_{n-1}(\delta^Y)$ is a non-central t distribution with $n-1$ degrees of freedom and non-centrality parameter $\delta^Y = 3\sqrt{n}C_I / \sqrt{1 + \tau^2}$. The mean, the variance, and the mean squared error of the estimator \tilde{C}_I^Y are

$$E(\tilde{C}_I^Y) = \frac{C_I}{\sqrt{1 + \tau^2}} \quad (4.5)$$

$$\text{Var}(\tilde{C}_I^Y) = \left\{ \frac{\Gamma((n-1)/2)\Gamma((n-3)/2)}{[\Gamma((n-2)/2)]^2} - 1 \right\} \frac{(C_I)^2}{1 + \tau^2} + \frac{\Gamma((n-1)/2)\Gamma((n-3)/2)}{9n[\Gamma((n-2)/2)]^2} \quad (4.6)$$

$$\begin{aligned} \text{MSE}(\tilde{C}_I^Y) &= \left(\frac{1}{\sqrt{1 + \tau^2}} - 1 \right)^2 (C_I)^2 + \left\{ \frac{\Gamma((n-1)/2)\Gamma((n-3)/2)}{[\Gamma((n-2)/2)]^2} - 1 \right\} \frac{(C_I)^2}{1 + \tau^2} \\ &\quad + \frac{\Gamma((n-1)/2)\Gamma((n-3)/2)}{9n[\Gamma((n-2)/2)]^2} \end{aligned} \quad (4.7)$$

For $\tau > 0$, \tilde{C}_I^Y is a biased estimator of C_I , and the bias $(1/\sqrt{1 + \tau^2} - 1)C_I$ decreases in τ . Since $\Gamma((n-1)/2)\Gamma((n-3)/2)/[\Gamma((n-2)/2)]^2 - 1$ is positive, then $\text{Var}(\tilde{C}_I^Y) < \text{Var}(\tilde{C}_I)$. To compare $\text{MSE}(\tilde{C}_I^Y)$ with $\text{MSE}(\tilde{C}_I)$, we consider the function $f(C_I, n, \tau) = \text{MSE}(\tilde{C}_I^Y) / \text{MSE}(\tilde{C}_I)$. By some reduction, we have $f(C_I, n, \tau) = 1$ if and only if

$$\tau = \frac{2\Gamma((n-2)/2)\sqrt{\Gamma((n-1)/2)\Gamma((n-3)/2) - [\Gamma((n-2)/2)]^2}}{2[\Gamma((n-2)/2)]^2 - \Gamma((n-1)/2)\Gamma((n-3)/2)} \quad (4.8)$$

or $\tau = 0$. Denote the right side of the equal sign in the above formula as τ_0 , we

have $f(C_I, n, \tau) > 1$ if $\tau > \tau_0$ and $f(C_I, n, \tau) < 1$ if $\tau < \tau_0$ exclusive of 0. It represents that $\text{MSE}(\tilde{C}_I^Y) > \text{MSE}(\tilde{C}_I)$ if $\tau > \tau_0$, $\text{MSE}(\tilde{C}_I^Y) < \text{MSE}(\tilde{C}_I)$ if $\tau < \tau_0$ exclusive of 0, and $\text{MSE}(\tilde{C}_I^Y) = \text{MSE}(\tilde{C}_I)$ if $\tau = \tau_0$ or 0.

Table 10. τ_0 values for $n = 5(5)100$.

n	τ_0	n	τ_0	n	τ_0	n	τ_0
5	1.439	30	0.279	55	0.199	80	0.163
10	0.587	35	0.255	60	0.189	85	0.157
15	0.431	40	0.237	65	0.181	90	0.153
20	0.356	45	0.222	70	0.174	95	0.149
25	0.310	50	0.209	75	0.168	100	0.145

Table 10 lists the τ_0 values for $n = 5(5)100$. Figures 16(a)-16(b) display the surface plots of the ratios $\gamma_4 = f(C_I, n, \tau)$ with $n = 5(1)100$ and τ in $[0, 1]$ for $C_I = 1.00$, and 1.33. The value τ_0 is greater than 0.5 for small n ($n \leq 10$), and greater than 0.2 for $n \leq 50$. When $50 < n \leq 100$, τ_0 is between 1.00 and 2.00. For large n , γ_4 is greater than 1 for almost every value of τ , and γ_4 increases if τ increases. The maximum values of γ_4 are 14.239, and 15.347, respectively, and the minimum values of γ_4 are 0.806 (1/1.241), and 0.797 (1/1.255), respectively. The maximum values of γ_4 occur at $n = 100$ and $\tau = 1$, and the minimum values of γ occur at $n = 5$ and $\tau = 0.788$. The difference between $\text{MSE}(\tilde{C}_I^Y)$ and $\text{MSE}(\tilde{C}_I)$ with $\gamma_4 > 1$ is more significant than that with $\gamma_4 < 1$.

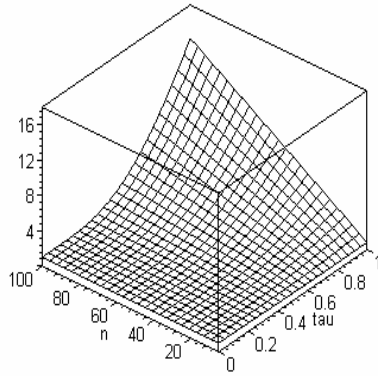


Figure 16(a). Surface plot of γ_4 with $n = 5(1)100$ and τ in $[0, 1]$ for $C_I = 1.00$.

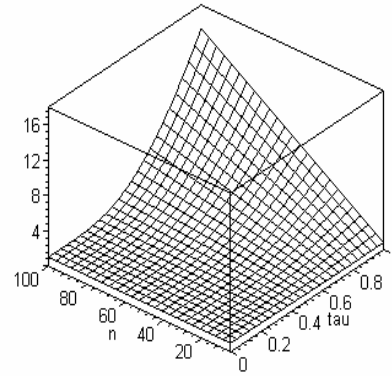


Figure 16(b). Surface plot of γ_4 with $n = 5(1)100$ and τ in $[0, 1]$ for $C_I = 1.33$.

4.3 Confidence Bounds Based on \tilde{C}_I^Y

The lower confidence bounds present a measure on the minimum capability of the process based on the sample data. Let $k_1 = 3\tilde{C}_{PU}/b_{n-1}$ and $k_2 = 3\tilde{C}_{PL}/b_{n-1}$, and we have $USL = \bar{X} + k_1S$ and $LSL = \bar{X} - k_2S$. A $100\theta\%$ lower confidence bound C_U for C_{PU} satisfies $P(C_{PU} \geq C_U) = \theta$. It can be

written as

$$\begin{aligned}
P(C_{PU} \geq C_U) &= P\left(\frac{USL - \mu}{3\sigma} \geq C_U\right) \\
&= P\left(\frac{\bar{X} + k_1 S - \mu}{3\sigma} \geq C_U\right) = P\left(\frac{Z - 3\sqrt{n}C_U}{S/\sigma} \geq -k_1\sqrt{n}\right) \\
&= P\left(\frac{Z - 3\sqrt{n}C_U}{S/\sigma} \geq -\frac{3\tilde{C}_{PU}}{b_{n-1}}\sqrt{n}\right) = P(t_{n-1}(\delta_U = -3\sqrt{n}C_U) \geq t_1) = \theta. \quad (4.9)
\end{aligned}$$

Similarly, a 100 θ % lower confidence bound C_L for C_{PL} satisfies $P(C_{PL} \geq C_L) = \theta$. It can be shown as $P(t_{n-1}(\delta_L = 3\sqrt{n}C_L) \leq t_2) = \theta$, where Z is distributed as Normal(0, 1), $t_1 = -k_1\sqrt{n}$, and $t_2 = k_2\sqrt{n}$. To find the exact 100 θ % lower confidence bounds, Pearn & Shu [40] provided an algorithm and a Matlab program to solve the above equations. With measurement errors, we use \tilde{C}_I^Y to estimate C_I but not \tilde{C}_I . Thus, $t_1^Y = -(3\tilde{C}_{PU}^Y/b_{n-1})\sqrt{n}$ and $t_2^Y = (3\tilde{C}_{PL}^Y/b_{n-1})\sqrt{n}$ instead of t_1 and t_2 , are substituted into the equations to obtain the confidence bounds. Denote the bounds originated from t_1^Y and t_2^Y as C_U^Y and C_L^Y . The confidence coefficient by the confidence bound C_U^Y (denoted by θ^Y) we obtained is

$$\begin{aligned}
\theta^Y &= P(C_{PU} \geq C_U^Y) = P\left(\frac{USL - \mu_Y}{3\sigma_Y} \sqrt{1 + \tau^2} \geq C_U^Y\right) \\
&= P\left(\frac{\bar{Y} + k_1^Y S_Y - \mu_Y}{3\sigma_Y} \geq \frac{C_U^Y}{\sqrt{1 + \tau^2}}\right) = P\left(\frac{Z - 3\sqrt{n}C_U^Y/\sqrt{1 + \tau^2}}{S_Y/\sigma_Y} \geq -k_1^Y\sqrt{n}\right) \\
&= P\left(\frac{Z - 3\sqrt{n}C_U^Y/\sqrt{1 + \tau^2}}{S_Y/\sigma_Y} \geq -\frac{3\tilde{C}_{PU}^Y\sqrt{n}}{b_{n-1}}\right) = P\left(t_{n-1}(\delta_U^Y = \frac{-3\sqrt{n}C_U^Y}{\sqrt{1 + \tau^2}}) \geq t_1^Y\right), \quad (4.10)
\end{aligned}$$

where $k_1^Y = 3\tilde{C}_{PU}^Y/b_{n-1}$. And, θ^Y can be also obtained by the confidence bound C_L^Y , which can be expressed as

$$\theta^Y = P\left(t_{n-1}(\delta_L^Y = \frac{3\sqrt{n}C_L^Y}{\sqrt{1 + \tau^2}}) \leq t_2^Y\right). \quad (4.11)$$

Figures 17(a)-17(b) plot θ^Y versus τ with $n = 25(25)100$ and $\tilde{C}_I = 1.00$, and 1.33, for 95% confidence intervals (because $E(\tilde{C}_I^Y) = E(\tilde{C}_I/\sqrt{1 + \tau^2})$, we consider the cases that $\tilde{C}_I^Y = \tilde{C}_I/\sqrt{1 + \tau^2}$). Since \tilde{C}_I^Y is smaller than \tilde{C}_I in the presence of measurement errors, and C_U^Y (or C_L^Y) is smaller than C_U (or C_L), it is necessary that θ^Y is always greater than θ . Thus, Figures 17(a)-17(b) show that the confidence coefficients become increase because the estimated lower confidence interval bounds become decrease by measurement errors.

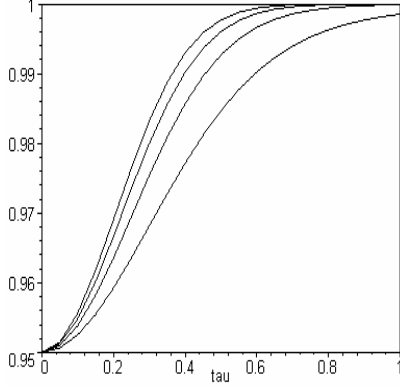


Figure 17(a). Plots of θ^Y versus τ with $\tilde{C}_I = 1.00$ and $n = 25(25)100$ (from top to bottom) for 95% confidence intervals.

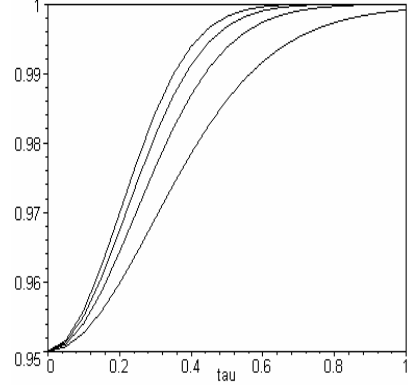


Figure 17(b). Plots of θ^Y versus τ with $\tilde{C}_I = 1.33$ and $n = 25(25)100$ (from top to bottom) for 95% confidence intervals.

4.4 Capability Testing Based on \tilde{C}_I^Y

We usually use statistical testing to determine if our processes meet the capability requirement. The null hypothesis is $H_0: C_I \leq c$ (process is not capable), and the alternative hypothesis is $H_0: C_I > c$ (process is capable) of testing, where c is our required process capability. The critical value is used to determine whether the null hypothesis should be rejected. If the point estimator of the process capability is greater than the critical value, we reject the null hypothesis and conclude that the process is capable. Otherwise, we would believe that the process is incapable. Suppose that the nominal size of our statistical testing is α (type I error), the critical value c_0 can be determined by

$$\alpha = P(\tilde{C}_I \geq c_0 | C_I = c). \quad (4.12)$$

Since \tilde{C}_I is distributed as $dt_{n-1}(\delta = 3\sqrt{n}C_I)$, where $d = b_{n-1}(3\sqrt{n})^{-1}$, we can obtain that c_0 is

$$c_0 = \frac{b_{n-1}}{3\sqrt{n}} t_{n-1, \alpha}(\delta = 3\sqrt{n}c), \quad (4.13)$$

where $t_{n-1, \alpha}(\delta)$ is the upper α th quantile of $t_{n-1}(\delta)$ distribution. And the power of the test can be calculated as

$$\begin{aligned} \pi(C_I) &= P(\tilde{C}_I > c_0 | C_I) = P(3\sqrt{n}\tilde{C}_I > 3\sqrt{n}c_0 | C_I) \\ &= P\left(\frac{3\sqrt{n}}{b_{n-1}} \tilde{C}_I > \frac{3\sqrt{n}}{b_{n-1}} c_0 | C_I\right) = P\left(t_{n-1}(\delta = 3\sqrt{n}C_I) > \frac{3\sqrt{n}}{b_{n-1}} c_0\right) \\ &= P(t_{n-1}(\delta = 3\sqrt{n}C_I) > t_{n-1, \alpha}(\delta = 3\sqrt{n}c)). \end{aligned} \quad (4.14)$$

However, in the presence of measurement errors, the α -risk (denoted by α^Y) and the power (denoted by π^Y) are

$$\begin{aligned}
\alpha^Y &= P(\tilde{C}_I^Y \geq c_0 | C_I = c) = P(3\sqrt{n}\tilde{C}_I^Y \geq 3\sqrt{n}c_0 | C_I = c) \\
&= P\left(\frac{3\sqrt{n}}{b_{n-1}}\tilde{C}_I^Y \geq \frac{3\sqrt{n}}{b_{n-1}}c_0 | C_I = c\right) = P\left(t_{n-1}(\delta^Y = 3\sqrt{n}C_I^Y) \geq \frac{3\sqrt{n}}{b_{n-1}}c_0 | C_I = c\right) \\
&= P\left(t_{n-1}(\delta^Y = 3\sqrt{n}\frac{c}{\sqrt{1+\tau^2}}) \geq t_{n-1,\alpha}(\delta = 3\sqrt{nc})\right). \tag{4.15}
\end{aligned}$$

$$\begin{aligned}
\pi^Y(C_I) &= P(\tilde{C}_I^Y > c_0 | C_I) = P(3\sqrt{n}\tilde{C}_I^Y > 3\sqrt{n}c_0 | C_I) \\
&= P\left(\frac{3\sqrt{n}}{b_{n-1}}\tilde{C}_I^Y > \frac{3\sqrt{n}}{b_{n-1}}c_0 | C_I\right) = P\left(t_{n-1}(\delta^Y = 3\sqrt{n}C_I^Y) > \frac{3\sqrt{n}}{b_{n-1}}c_0 | C_I\right) \\
&= P\left(t_{n-1}(\delta^Y = 3\sqrt{n}\frac{C_I}{\sqrt{1+\tau^2}}) > t_{n-1,\alpha}(\delta = 3\sqrt{nc})\right). \tag{4.16}
\end{aligned}$$

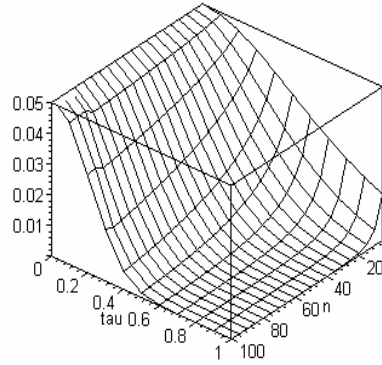
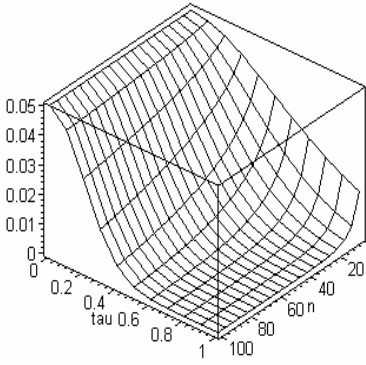


Figure 18(a). Surface plot of α^Y with $n = 5(1)100$, τ in $[0, 1]$ for $c = 1.00$, $\alpha = 0.05$.

Figure 18(b). Surface plot of α^Y with $n = 5(1)100$, τ in $[0, 1]$ for $c = 1.33$, $\alpha = 0.05$.

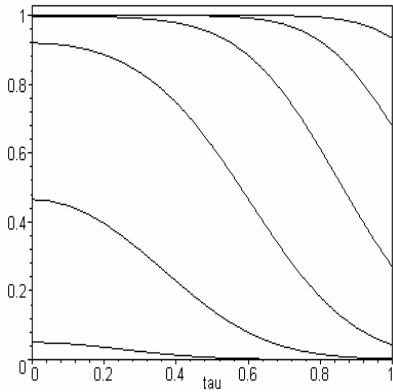


Figure 19(a). Plots of π^Y versus τ , with $n = 50$, $\alpha = 0.05$, for $c = 1.00$, $C_I = 1.00(0.20)2.00$ (from bottom to top).

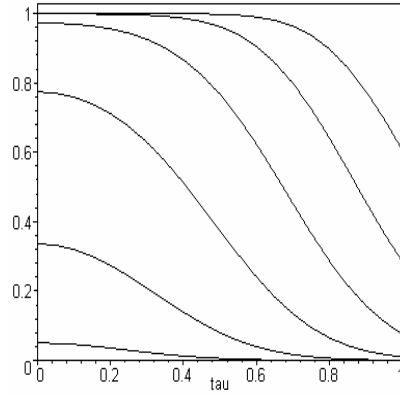


Figure 19(b). Plots of π^Y versus τ , with $n = 50$, $\alpha = 0.05$, for $c = 1.33$, $C_I = 1.33(0.20)2.33$ (from bottom to top).

Earlier discussions indicate that we underestimate the true process

capability using \tilde{C}_I^Y instead of \tilde{C}_I . The probability that \tilde{C}_I^Y is greater than c_0 would be less than that of using \tilde{C}_I . Thus, the α -risk using \tilde{C}_I^Y to estimate C_I is less than the α -risk if using \tilde{C}_I to estimate C_I . The power, if using \tilde{C}_I^Y to estimate C_I , is also less than the power using \tilde{C}_I . That is, we have $\alpha^Y \leq \alpha$ and $\pi^Y \leq \pi$. Figures 18(a)-18(b) are the surface plots of α^Y with $n = 5(1)100$ and τ in $[0, 1]$ for $C_I = 1.00, 1.33$ and $\alpha = 0.05$. Figures 19(a)-19(b) are the plots of π^Y versus τ with $n = 50$ and $\alpha = 0.05$ for $c = 1.00, 1.33$ and $C_I = c(0.20)c + 1$. Note that for $\tau = 0$, $\alpha^Y = \alpha$ and $\pi^Y = \pi$ in those figures. In Figures 18(a)-18(b), α^Y decreases as τ or n increases, and the decreasing rate is more significant with large c values. We find that for large τ values α^Y is smaller than 1×10^{-5} . In Figures 19(a)-19(b), π^Y decreases as τ increases, but increases as n increases. Decrement of π^Y by τ is more significant for large c values. Because of measurement errors, π^Y may decrease significantly. For instance, in Figure 19(a) the π^Y values ($c = 1.00, n = 50$) for $C_I = 1.40$ is $\pi^Y = 0.920$ if there is no measurement error ($\tau = 0$). But, when $\tau = 1.0$, π^Y decreases to 0.042, the decrement of the power is 0.878.

4.5 Modified Confidence Bounds and Critical Values

We showed earlier that the coefficients increase owing to the underestimating the lower confidence bounds. We also showed that both the α -risk and the power of the test decrease in measurement error. The probability of passing non-conforming product units decreases, but the probability of correctly judging a capable process as incapable also decreases. Since the lower confidence bound of the process capability is severely underestimated, and the power becomes much weak, the producers cannot firmly state that their processes meet the capability requirement even if their processes are sufficiently capable. Good product units would be incorrectly rejected in this case (rejected products are either scrapped or requiring rework). Unnecessary cost may accompany those incorrect decisions to the producers. Improving the gauge capability and training the operators by proper education are some advice for reducing the measurement errors. Nevertheless, measurement errors may be unavoidable in most manufacturing processes. Thus in this section, we adjust the confidence bounds to give a more precise estimation of process capability, and revise critical values to improve the power for testing hypothesis.

Suppose that the desired confidence coefficient is θ , the adjusted confidence interval of C_{PU} with confidence interval bound C_U^* , can be established as

$$\theta = P\left(C_{PU} \geq C_U^*\right) = P\left(\frac{USL - \mu_Y}{3\sigma_Y} \sqrt{1 + \tau^2} \geq C_U^*\right).$$

$$\begin{aligned}
&= P\left(\frac{\bar{Y} + k_1^Y S_Y - \mu_Y}{3\sigma_Y} \geq \frac{C_U^*}{\sqrt{1+\tau^2}}\right) = P\left(\frac{Z - 3\sqrt{n}C_U^* / \sqrt{1+\tau^2}}{S_Y / \sigma_Y} \geq -k_1^Y \sqrt{n}\right) \\
&= P\left(\frac{Z - 3\sqrt{n}C_U^* / \sqrt{1+\tau^2}}{S_Y / \sigma_Y} \geq -\frac{3\tilde{C}_{PU}\sqrt{n}}{b_{n-1}}\right) = P\left(t_{n-1}(\delta_U^* = \frac{-3\sqrt{n}C_U^*}{\sqrt{1+\tau^2}}) \geq t_1^Y\right). \quad (4.17)
\end{aligned}$$

Similarly, the adjusted confidence interval of C_{PL} with confidence interval bound C_L^* , can be established as

$$\theta = P\left(t_{n-1}(\delta_L^* = \frac{3\sqrt{n}C_L^*}{\sqrt{1+\tau^2}}) \leq t_2^Y\right). \quad (4.18)$$

To find the exact $100\theta\%$ lower confidence bounds, an S-plus program is developed to solve the equations. Figures 20(a)-20(b) are comparisons among C_U , C_U^Y , and C_U^* for $\tilde{C}_{PU} = 1.00, 1.33$ with $n = 50$, where C_U is the 95% lower confidence bound of \tilde{C}_{PU} , C_U^Y is the 95% lower confidence bound of \tilde{C}_{PU}^Y , and C_U^* is the adjusted 95% lower confidence bound for \tilde{C}_{PU}^Y . Note that in this case, the probability that the interval with the bound C_U^Y contains the actual C_{PU} value is greater than that of the interval with the bound C_U or C_U^* does, while the probability that the interval with the bound C_U or C_U^* contains the actual C_{PU} value is just 0.95. From Figures 20(a)-20(b), we see that the lower confidence bounds remained underestimated, even if we adjust the formula to calculate the bounds. But, the magnitude of underestimation using adjusted confidence bounds is significantly reduced.

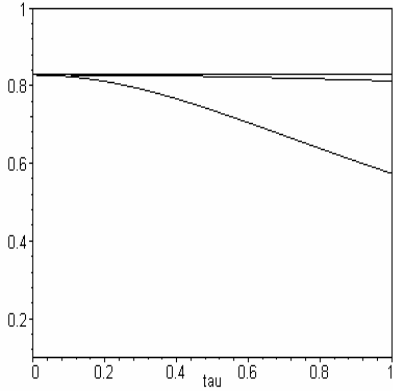


Figure 20(a). Plots of C_U , C_U^* , and C_U^Y (from top to bottom) versus τ with $n = 50$ and for $\tilde{C}_{PU} = 1.00$.

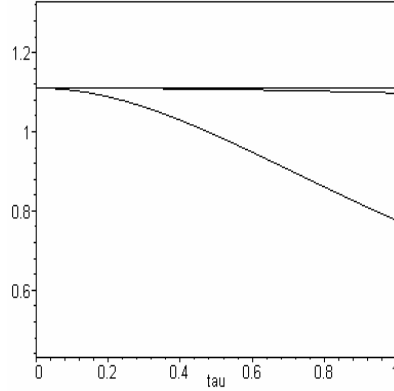


Figure 20(b). Plots of C_U , C_U^* , and C_U^Y (from top to bottom) versus τ with $n = 50$ and for $\tilde{C}_{PU} = 1.33$.

In order to improve the power of the test, we consider the revised critical values c_0^* satisfied $c_0^* < c_0$. Thus, the probability that \tilde{C}_I^Y is greater than c_0^* is greater than the probability that \tilde{C}_I^Y is greater than c_0 . Both the α -risk and the power increase when we use c_0^* as a new critical value in the testing. Suppose that the α -risk using the revised critical value c_0^* is α^* , the revised critical c_0^* must satisfy

$$\begin{aligned}
\alpha^* &= P\left(\tilde{C}_I^Y \geq c_0^* \mid C_I = c\right) = P\left(3\sqrt{n}\tilde{C}_I^Y \geq 3\sqrt{n}c_0^* \mid C_I = c\right) \\
&= P\left(\frac{3\sqrt{n}}{b_{n-1}}\tilde{C}_I^Y \geq \frac{3\sqrt{n}}{b_{n-1}}c_0^* \mid C_I = c\right) = P\left(t_{n-1}(\delta^Y = 3\sqrt{n}C_I^Y) \geq \frac{3\sqrt{n}}{b_{n-1}}c_0^* \mid C_I = c\right) \\
&= P\left(t_{n-1}(\delta^Y = 3\sqrt{n}\frac{c}{\sqrt{1+\tau^2}}) \geq \frac{3\sqrt{n}}{b_{n-1}}c_0^*\right). \tag{4.19}
\end{aligned}$$

To ensure that the α -risk is within the preset magnitude, we let $\alpha^* = \alpha$, thus c_0^* can be obtained as

$$c_0^* = \frac{b_{n-1}}{3\sqrt{n}}t_{n-1,\alpha}\left(\delta^Y = 3\sqrt{n}\frac{c}{\sqrt{1+\tau^2}}\right), \tag{4.20}$$

and the power π^* is

$$\begin{aligned}
\pi^*(C_I) &= P\left(\tilde{C}_I^Y > c_0^* \mid C_I\right) = P\left(3\sqrt{n}\tilde{C}_I^Y > 3\sqrt{n}c_0^* \mid C_I\right) \\
&= P\left(\frac{3\sqrt{n}}{b_{n-1}}\tilde{C}_I^Y > \frac{3\sqrt{n}}{b_{n-1}}c_0^* \mid C_I\right) = P\left(t_{n-1}(\delta^Y = 3\sqrt{n}C_I^Y) > \frac{3\sqrt{n}}{b_{n-1}}c_0^* \mid C_I\right) \\
&= P\left(t_{n-1}(\delta^Y = 3\sqrt{n}\frac{C_I}{\sqrt{1+\tau^2}}) > t_{n-1,\alpha}\left(\delta^Y = 3\sqrt{n}\frac{c}{\sqrt{1+\tau^2}}\right)\right). \tag{4.21}
\end{aligned}$$

Figures 21(a)-21(b) plot π^* versus τ with $n = 50$ and $\alpha = 0.05$ for $c = 1.00, 1.33$, and $C_I = c(0.20)c + 1$. From those figures, we see that the powers corresponding to the adjusted critical values c_0^* remain decreasing in measurement error, but the decrements originated from the new critical values c_0^* are very small. We have improved a certain degree of power. For instance, if we compare the π^Y values in Figure 19(a) ($c = 1.00, n = 50$) for $C_I = 1.40$ with the π^* values in Figure 21(a) ($c = 1.00, n = 50$) for $C_I = 1.40$, we see that $\pi^Y = 0.042$ and $\pi^* = 0.885$ with $\tau = 1.0$. In this case, using the adjusted critical values c_0^* the power is improved by 0.843. Tables 20-23 in Appendix provide the revised critical values for some commonly used capability requirements. Using those tables, the practitioner may select the proper critical values for capability testing.

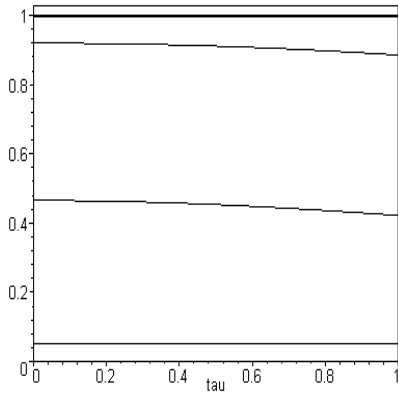


Figure 21(a). Plots of π^* versus τ , with $n = 50$, $\alpha = 0.05$, for $c = 1.00$, $C_I = 1.00(0.20)2.00$ (from bottom to top).

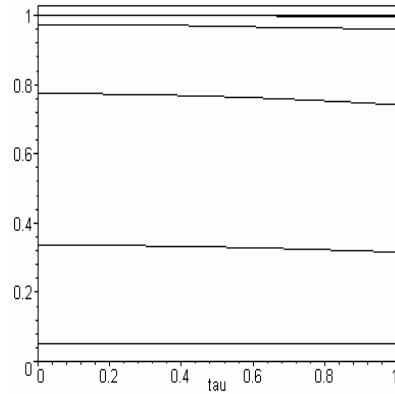


Figure 21(b). Plots of π^* versus τ , with $n = 50$, $\alpha = 0.05$, for $c = 1.33$, $C_I = 1.33(0.20)2.33$ (from bottom to top).

4.6 Application Example

TFT-LCDs (thin-film-transistor liquid crystal display) consist of a lower glass plate on which the TFT is formed, an upper glass plate on which the color filter is formed, and the injected liquid crystal between both glass plates (see Figure 22(a)). The TFT plays a critical role in transmitting and controlling electric signals, which determines the amount of voltage applied to the liquid crystal. The liquid crystal controls light permeability using different molecular structures that vary in accordance with the voltage. In this way, the desired color and image is displayed as it passes through the color filter (see figure 22(b)). The TFT-LCD consumes less energy compared to a CRT (cathode-ray tube), is slimmer and weighs less. The TFT-LCD emerges as the most widely used display solution, because of its high reliability, viewing quality and performance, compact size and environment- friendly features. Because of the heat resistance, non-conductance, and simple processing steps. Non-alkali thin film glass is the major material of manufacturing TFT-LCD. While manufacturing non-alkali thin film glass, flatness is one of the critical quality characteristics. If the flatness of glass is not in control, the TFT-LCD products may result in a certain degree of chromatic aberration.

Table 11. 60 observations for flatness (unit: μm)

14.40	4.47	11.18	8.29	9.38	8.73	11.64	6.59	12.55	12.83	14.40
12.18	14.73	12.22	10.42	11.56	14.37	11.76	8.06	10.03	5.45	12.18
14.40	15.28	9.60	15.01	12.36	14.69	10.71	6.96	8.88	16.30	14.40
15.53	15.22	12.02	12.95	10.50	15.09	11.23	8.33	13.76	12.19	15.53
9.93	9.14	10.41	15.34	12.94	10.24	14.44	12.54	10.40	13.47	9.93
13.22	16.93	18.41	11.19	15.09	9.40	12.22	12.17	13.80	12.60	13.22

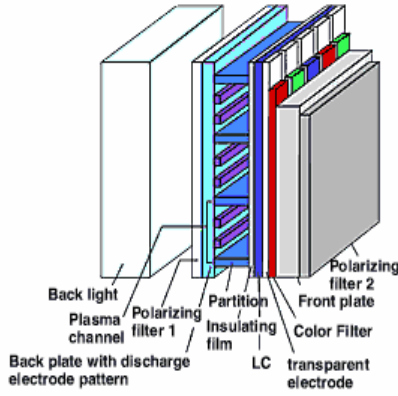


Figure 22(a). Structure of TFT-LCD (a).

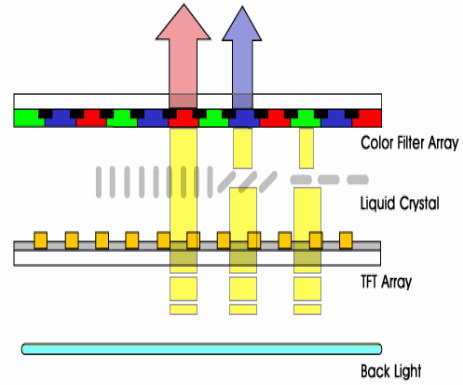


Figure 22(b). Structure of TFT-LCD (b).

Consider a supplier in manufacturing TFT-LCD products in Taiwan, the production specifications of flatness for a particular model of non-alkali thin film glass are: $USL = 25 \text{ } \mu\text{m}$ (0.0025 mm), $T = 0 \text{ } \mu\text{m}$. A total of 60 observations were collected which are displayed in Table 11. To determine whether the process is “Satisfactory” ($C_{PU} > 1.33$) with unavoidable measurement errors $\tau = 0.4$, we propose the following procedure, STEP 1: Determine the capability requirement c (normally chosen to 1.00, 1.33, 1.50) and the α -risk (normally set to 0.01, 0.025, or 0.05), STEP 2: Calculate the value of the point estimator \tilde{C}_I from the sample, STEP 3: Check the appropriate table listed in Tables 20-23 and finding the corresponding critical value c_0^* based on α , τ , and n , STEP 4: Conclude that the process meets the capability requirement if \tilde{C}_I is greater than c_0^* . Otherwise, we do not have enough information to conclude that the process is capable.

With the proposed procedure, we first determine that $c = 1.33$ and $\alpha = 0.05$. Based on the sample data of 60 observations, we obtain the sample mean $\bar{Y} = 11.93$, the sample standard deviation $S_Y = 2.85$, and the point estimator $\tilde{C}_{PU}^Y = 1.511$. From Table 22, we find the critical value $c_0^* = 1.452$ based on α , τ and n . Since $\tilde{C}_{PU}^Y > c_0^*$, we conclude that the process is “Satisfactory”. Moreover, by inputting \tilde{C}_{PU}^Y , τ , n , and the desired confidence coefficient $\theta = 0.95$ into the computer program we can obtain the 95% lower confidence bound of this process capability as 1.385.